Engineering Transactions, **73**(3): 387–405, 2025, https://doi.org/10.24423/engtrans.3471.2025
Institute of Fundamental Technological Research Polish Academy of Sciences (IPPT PAN)
Université de Lorraine • Poznan University of Technology

SiMRTRANS

Research on Liquid Flow Resistance in Flow and Centrifugal Extraction Reactors

Jędrzej MĄCZAK, Dmytro SAMOILENKO, Michał MAKOWSKI*, Lech KNAP

Institute of Vehicles and Construction Machinery Engineering
Warsaw University of Technology
Warsaw, Poland; e-mails: jedrzej.maczak@pw.edu.pl, dmytro.samoilenko@pw.edu.pl, Lech.Knap@pw.edu.pl

*Corresponding Author e-mail: michal.makowski1@pw.edu.pl

This paper presents research that formed the basis for the development of a low-temperature centrifugal extraction reactor. This reactor is used to obtain medicinal substances from herbs, where key parameters include extraction time, temperature, and the velocity of the solvent that flows through the dried herbs. An important parameter for performing simulation studies was the assessment of the medium flow characteristics through the dried medicinal herb material. For this purpose, a flow reactor was developed and tested.

The first part of the paper discusses the results of numerical and experimental studies on liquid flow through the extraction reactor. This part of the work was carried out in order to determine the parameters related to the resistance of liquid flow through dried medicinal herbs. This resistance of the liquid flow through the herbs affects the limitation of its velocity and has a direct impact on the efficiency of the process. In the second part of the paper, the results obtained from the flow reactor experiments were used for numerical investigations of the centrifugal extractor drum.

Keywords: extraction reactor; numerical investigations; flow resistance; medicinal herbs.

1. Introduction

The research topic is related to the design of devices used for extracting oil-based substances from medicinal herbs. The extraction process yields raw materials utilized in the pharmaceutical and cosmetic industries. Solutions with specific pH values, which act as solvents, are used in the extraction. In the pharmaceutical industry, these solvents allow the extraction of pharmacologically active substances, often of natural origin, such as those found in medicinal

herbs. Commonly used solvents include water, methanol, ethanol acetone, ether, and chloroform [1–5]. Depending on the production scale or the nature of the research, various extraction methods are employed, including Soxhlet extraction, surface extraction, ultrasound-assisted extraction, and microwave-assisted extraction [1, 2, 4, 6].

The research presented in this paper was conducted to obtain parameters for the design of a centrifugal extraction reactor. Devices of this type are used in research and in the pharmaceutical industry. One of the main advantages of this method, compared to traditional methods such as maceration, is the reduced time required to obtain the desired substance. Previous studies using centrifugal extractors have been presented in [1, 7, 8].

A problem that arises in the extraction process is related to the dissolution of various contaminants in the final product. These may include solid impurities (soil, sediments, and dust), as well as chloroorganic and organophosphorus contaminants (pesticides), polychlorinated biphenyls, and dioxins [1]. Additionally, at elevated temperatures (around 31°C), the decomposition of thermally unstable compounds occurs [9]. A solution to this is to conduct the extraction at negative temperatures, around or below −30°C. Under such conditions, the solubility of contaminants in the solvent can be minimized, while dissolution efficiency of target compounds, such as cannabidiol (CBD) and cannabidiolic acid (CBDA) [10], remains high. A preliminary design of the setup used for studies with a flow reactor was presented in [11, 12].

The study of liquid flow through dried medicinal herbs is largely based on the results of experimental studies, due to the challenges that arise when modeling porous media [13, 14]. In the case of studies on solvent flow through a container filled with dried herbs, it can be assumed that flow resistance will be similar to that observed in filter studies in hydraulic systems. For example, [15] presents the results of numerical studies on liquid flow through a filter. An additional complexity in the design process involves heat transfer from the surroundings to the solvent. Numerical studies related to pump selection for the cooling system are presented in [16]. Meanwhile, studies such as [17, 18] focus on heat exchange process between the liquid flowing through the pipes and the surrounding environment. In these studies, the heat flows from the liquid being tested to the surroundings, whereas in the present case, the heat flow is reversed, with heat entering the solvent from the external environment.

This paper describes the construction of a research setup that serves as a flow extractor, used to determine the operating parameters of a low-temperature extraction reactor. In the target solution, ethanol is used as the solvent, and the process is conducted at −30°C. At such low temperatures, the process of dissolving impurities in the extract does not occur. The analyses conducted indicate that the extraction process should take about 15 minutes, as this duration al-

lows for a relatively high concentration of desired substances (e.g., CBD) while maintaining a low level of impurities. The efficiency of the extraction process can be improved by forcing the solvent to flow through the medicinal herb material. For this reason, studies were undertaken to investigate the flow resistance of the liquid through the herb material, as this directly affects the flow velocity. An analysis was also carried out on the impact of the herb mass and the thickness of the herb layer on flow velocity.

The aim of the numerical studies on the centrifugal reactor was to determine parameters describing the flow characteristics of liquid through solid material. Therefore, in the first phase of the research, a model of the container filled with solid material in the form of a porous body was developed. The determined liquid flow rate was then compared to experimental results obtained for liquid flow through the solid material. The parameters obtained from this comparison were used in further studies analyzing fluid dynamics in the centrifugal extraction reactor. This paper presents selected research results, taking into account the porous body model parameters and process parameters to achieve high extraction efficiency.

The work is divided into six sections. The introduction presents issues related to the process of extracting medicinal substances from medicinal herbs and outlines the objectives of the research. Section 2 presents the concept and construction of the flow extraction reactor. Section 3 covers the experimental studies on the flow extractor, including selected research results. Section 4 discusses the numerical analysis of the flow extractor, focusing on the determination of flow parameters through the porous medium. Section 5 is dedicated to the numerical studies of the centrifugal extraction reactor, presenting research conducted using a centrifuge drum model. The final section, Sec. 6, provides a summary of the research conducted and outlines directions for future studies.

2. Construction of the measurement test bed for the flow reactor

The schematic concept of the research test bed developed for the flow reactor used in extracting medicinal substances from herbs is shown in Fig. 1. The diagram includes a container with dried herbs (1), through which the solvent flows. The solvent flow is driven by a pump (2). The solvent is drawn from a storage tank (3), and returns to it after passing through the dried material. The hydraulic system is protected from excessive pressure by a safety valve (4). The extraction process begins when valve (5) is opened, and the process parameters: pressure, flow rate, and temperature are recorded by a pressure transducer (6), a flow rate sensor (7), and a thermocouple for temperature measurement (8), respectively.

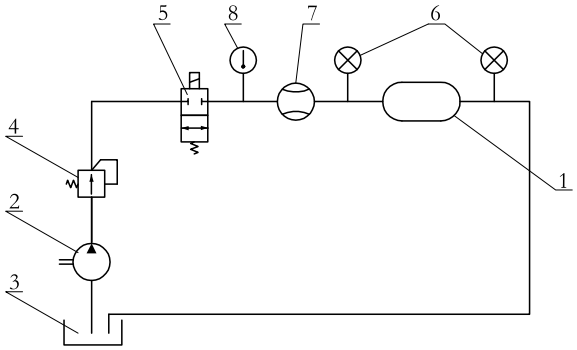

FIG. 1. Schematic concept of the extraction station.

Based on the presented concept, a model of the laboratory test bed was developed, as shown in Fig. 2 (designed using CATIA V5 software). The container filled with dried material (1) is placed at the same level as the pump (2), which generates the solvent flow. The solvent is stored in a tank (3) and flows to the pump via a supply line (4), then passes through the herb container, and returns to the tank through an outlet line (5). It is assumed that the liquid flow rate in the test station is manually controlled by a valve (6). Excess solvent is returned to the tank through this valve. This valve also serves to cut off the solvent flow to the dried material before starting tests. The liquid flow rate through the herb container is measured by a sensor (7). The container is a cylinder with a diameter of 40 mm, and the liquid flow speed through the dried material is determined based on the measured flow rate. The pressure difference before and after the container with dried material is measured by pressure transducers (8). The system also includes a temperature sensor to monitor changes in liquid temperatures during tests at sub-zero temperatures.

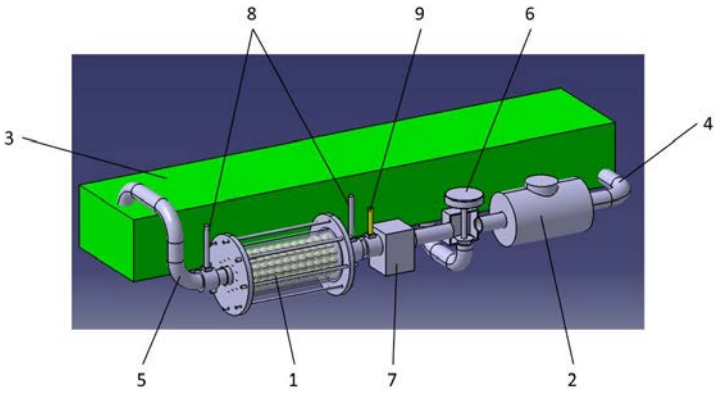

FIG. 2. Design of a test bed for a flow reactor.

During the design process, various positions of the individual system components relative to each other were considered. This primarily involved the relative positioning of the solvent tank, pump, and container with dried material. In the proposed solution, a single valve was sufficient to isolate the dried material container from the liquid, thereby simplifying the flow control process. An alternative design, in which the pump would draw liquid from the tank by creating a vacuum, was also considered; however, this approach posed the risk of air entering the pump. The proposed solution is both straightforward and effective, successfully fulfilling the intended function of the developed system.

As a result of the conceptual and design work, a laboratory test bed was built, as shown in Fig. 3. The key components of the setup include: the dried material container (1), pump (2), solvent tank (3), control valves (4), flow meter (5), pressure transducers (6), temperature sensor (7), measurement cards (8), measurement computer (9), and sensor power supply (10). The liquid flow was driven by a MAGNA 25–100 pump, with a maximum flow rate of 10 dm^3/min and a discharge pressure of 0.1 MPa. The flow rate of liquid passing through the dried material was determined based on readings from the flow sensor (5), flow resistance was measured using the pressure difference from the transducers (6), and temperature control was achieved via a thermocouple (7). Measurement data obtained from sensors were recorded on a computer (9), where custom software developed on the LabVIEW platform was installed. Signals from the sensors were processed using National Instruments measurement cards (8), while the sensors were powered by an electronic power system (10).

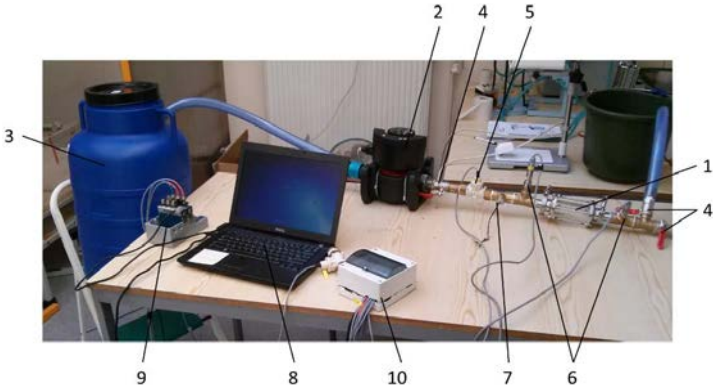

Fig. 3. General view of the measurement test bed for flow property testing.

The dried herbs in the container were enclosed on both sides with screens designed to prevent mechanical impurities from entering the solvent during the extraction process. Tests were conducted to estimate the flow resistance introduced by different types of screens with varying mesh sizes: 20, 60, 100, and

200 mesh. Among these, mesh 20 had the fewest openings (largest pores), while mesh 200 had the highest number of openings per unit area (smallest pores). Preliminary tests were conducted without the dried material using different screen types. A pressure drop of approximately 0.0033 MPa was observed for both mesh 20 and mesh 200 [11]. The mesh size was crucial, as solid particles carried with the liquid could act as contaminants or accumulate on sensors and other hydraulic system components, potentially affecting measurement accuracy and system performance.

3. Experimental studies on the resistance of the flow reactor

The flow resistance tests were conducted using dried hop material, which will later be replaced by dried medicinal herbs in subsequent studies. In the first phase of testing, water was used as the solvent, while the target solvent will be ethyl alcohol, chosen for its ability to retain properties at low temperatures.

The aim of the conducted research was to determine the flow resistance for different masses and thicknesses of the dried material layer, which vary according to the mass of the dried material in the container. Tests were carried out with liquid flowing through dried material masses of 5 g, 7.5 g, 10 g, and 12.5 g. During the measurements, the flow rate and pressure were measured, and temperature was also monitored. With the use of liquid at ambient temperature, temperature changes were minimal as a result of pressure fluctuations, while more significant changes were observed due to the pump's operation. The influence of temperature on changes in the liquid flow resistance was excluded from the tests since the temperature remained constant. During the tests, the duration of the tests was also measured, as extraction time relates to the efficiency of the process, as well as the level of contaminants dissolved in the liquid. Additionally, the dried herbs undergo maceration, which alters their mass and volume due to liquid absorption.

Before starting the measurements, the dried material of the specified mass was placed in the container, and then the pump was turned on and the valve opened to allow the solvent to flow through the dried material. During the flow, the thickness of the dried material layer changed, as illustrated in Figs. 4 and 5. Figure 4a shows the 12 g of dried material at the beginning of the experiment and Fig. 4b shows it after about 5 minutes of flow. Similarly, Figs. 5a and 5b depict the container with 5 g of dried material at the beginning of the measurement and after about 5 minutes of flow, respectively. In both cases, the change in layer thickness directly influenced an increase in flow resistance and a corresponding change in flow speed. The visible change in layer thickness consequently influenced these flow parameters.

a) b)

FIG. 4. View of the container filled with 12.5 g of dried material:
a) start of the flow, b) change in the thickness of the dried material layer.

a) b)

FIG. 5. View of the container filled with 5 g of dried material:
a) start of the flow, b) change in the thickness of the dried material layer.

The paper presents example results from the experimental studies. Figure 6 shows the results of liquid flow through 5 g of dried material, where pressure

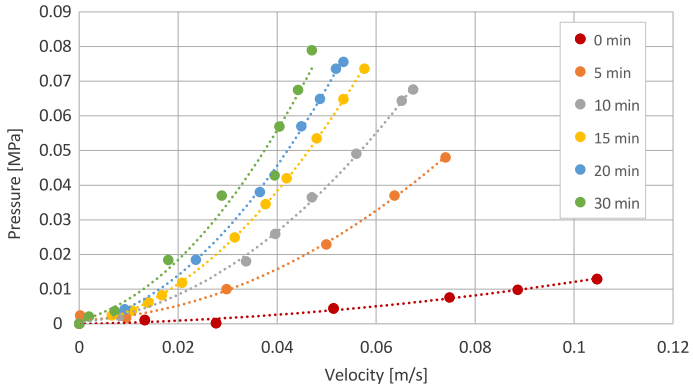

FIG. 6. Pressure difference in the hydraulic system with 5 g of dried material as a function of changes in liquid flow velocity.

changes are visible as a function of flow velocity, comparing the results at the start of the measurement (0 min) and after flow durations of 5 min, 10 min, 15 min, 20 min, and 30 min. It can be observed that at the beginning of the measurement, the pressure difference between the inlet and outlet of the container with the dried material is the lowest, and after 5 minutes, there is a sharp increase in flow resistance, which corresponds with a reduction in flow velocity. The greatest flow resistance, accompanied by smaller changes, occurs between 20 and 30 minutes of measurement time. The maximum pressure difference is 0.08 MPa, while the flow velocity decreases to 0.045 m/s. After 15 minutes, identified as the time to achieve satisfactory extraction efficiency with an acceptable level of contaminants, the flow resistance was about 0.75 MPa and the flow velocity was approximately 0.055 m/s.

Figure 7 shows pressure changes during liquid flow through 12.5 g of dried material. In this case, the tests are presented over a shorter maceration time range for the dried material: at the start of the experiment (0 min), and after 5 min, 10 min, and 15 min. It can be observed that at the beginning of the experiment (0 min), the pressure difference is the lowest, but after 15 minutes of flow, the pressure difference increases slightly. In the case of flow velocity, similarly to the dried material with a mass of 5 g, the velocity decreases by 2/3 during the 0–15 minute period. The maximum pressure difference is 0.09 MPa, with a flow velocity of 0.009 m/s.

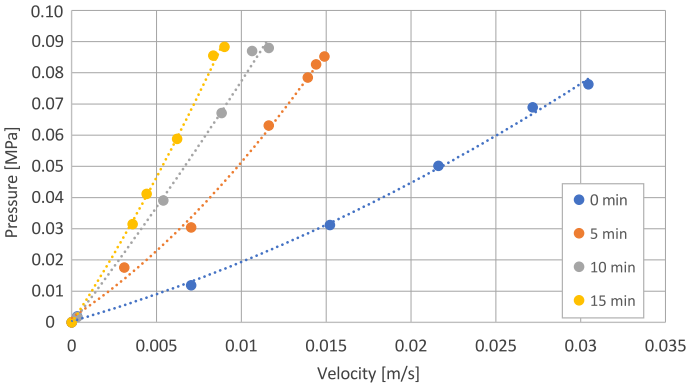

Fig. 7. Pressure difference in the hydraulic system with 12.5 g of dried material as a function of changes in liquid flow velocity.

The results of tests conducted at a flow time of 15 minutes with different masses of dried material in the container are shown in Fig. 8.

The figure shows changes in the pressure difference values, with the largest increases in pressure occurring when the dried material mass increases from 5 g to 10 g, while the smallest changes occur between 10 g to 12.5 g. Similar

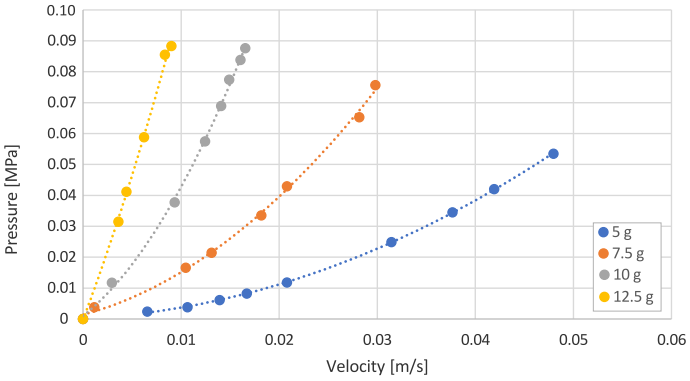

Fig. 8. Pressure difference in the hydraulic system after 15 minutes of flow time through dried material of varying masses as a function of flow velocity.

changes are observed in the flow velocity. This is related to the maceration of the dried material and changes in its structure, which contribute to increased flow resistance.

4. Numerical studies of the flow reactor

The results of the experimental studies were used to determine the parameters for the numerical model of the flow extractor. In the next stage, these research results will serve as the basis for simulation studies of the centrifugal extractor model. It was assumed that the dried material filling the container could be modeled as a porous medium. In the adopted model, the pipe lengths correspond to the locations of the pressure sensors, and the cylindrical section of the container is filled with the dried material model, where a layer thickness corresponds to that used in the experimental studies.

Figure 9 presents the numerical model of the setup used to measure flow resistance through dried material. In the numerical studies, similarly to the experimental studies, part of the container space is filled with dried material. This model was adopted to determine the flow resistance of the liquid through dried material at different masses and flow times, where flow time directly corresponds to the maceration time of the dried material. The paper presents example

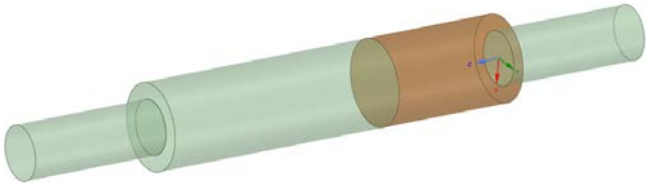

Fig. 9. Numerical model used for flow resistance studies.

numerical results corresponding to the experimental studies under the following conditions:

- mass of dried material; 5 g with layer thickness of 32–36 mm,
- mass of dried material; 7.5 g with layer thickness of 52–67 mm,
- mass of dried material; 12.5 g with layer thickness of 91–93 mm.

Figure 10 shows the computational mesh of the container with dried material, modeled in the ANSYS software. The numerical studies based on this mesh enable determination of the velocity and pressure distribution of the liquid flow through the container. For the simulation studies, initial parameters related to the viscosity and inertia of the liquid must be specified, from which viscous and inertial flow resistance coefficients are defined. In the simulation studies, the dried material is modeled as a porous medium. The ANSYS/Fluent software includes a module that describes a porous flow media, where flow resistance coefficients through the porous body are incorporated by modifying the Navier–Stokes with an additional term [19]:

$$\frac{\partial}{\partial t}(\rho \mathbf{v}) + \nabla(\rho \mathbf{v}) = -\nabla p + \nabla\left(\overline{\overline{\tau}}\right) + \rho \mathbf{g} + \mathbf{F}, \tag{4.1}$$

where ρ – liquid density, $\mathbf{v}$ – flow velocity, p – pressure, $\mathbf{F}$ – inertial force, ∇ – Laplace operator, τ – shear stress, and $\mathbf{g}$ – gravitational acceleration.

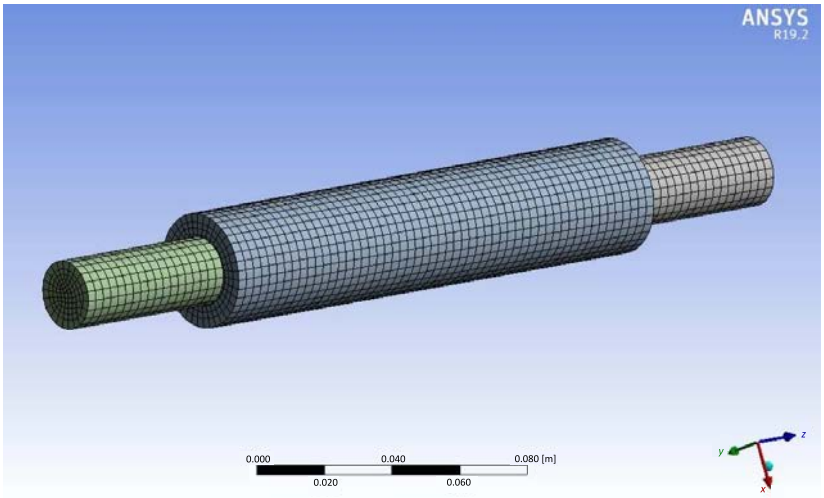

FIG. 10. Simulation model of the container with dried material – computational mesh.

In the porous body model, the software uses an external function that was determined based on the Darcy–Forchheimer equation. This relationship represents the flow resistance force (S_i), which depends on pressure changes relative to

the position within the porous material. This force is determined based on the following relationship [19]:

$$\frac{\Delta p}{\Delta x_i} = S_i = -\frac{\mu}{\alpha} v_i + 0.5 C_2 \rho \left| v \right| v_i, \tag{4.2}$$

where α, C_2 – parameters representing the viscous and inertial flow resistance coefficients, Δp – pressure drop, μ – dynamic viscosity, and Δx_i – position change along direction i.

The viscous and inertial resistance coefficients for the porous material were determined based on experimentally obtained approximated pressure drop against velocity characteristics for the studied material. In this context, the following parabolic function was used:

$$\Delta p = a v_i^2 - b v_i. \tag{4.3}$$

Thus, the viscous and inertial resistance coefficients were calculated from the following formulas:

$$\frac{1}{\alpha} = \frac{b}{\mu \Delta x_i} \tag{4.4}$$

and

$$C_2 = \frac{2a}{\rho \Delta x_i}. \tag{4.5}$$

The presented resistance coefficients, aligned with the direction of liquid flow, characterize the linear and nonlinear pressure drops across the porous material. These coefficients were determined based on the experimental studies presented in the previous section. The developed model of the dried material and the derived parameters will be validated in subsequent flow phases based on the experimental studies conducted.

Numerical studies were also carried out using the dried material model with a mass of 12.5 g. The results for the liquid flow time through the dried material after 2 minutes are shown in Fig. 11, depicting the pressure distribution, and in Fig. 12, showing the velocity magnitude distribution.

In the case of numerical studies of liquid flow through dried material with a mass of 12.5 g after 2 minutes, the pressure distribution, similar to the previous findings, shows a maximum pressure of 0.19 MPa and a pressure difference of approximately 0.09 MPa. The maximum velocity magnitude was determined to locally reach 1.37 m/s, while in the region containing the dried material, the velocity dropped to lower values.

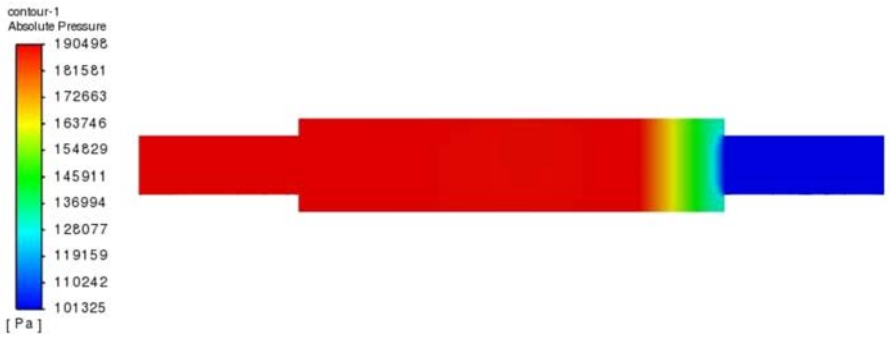

Fig. 11. Pressure distribution from numerical simulations of liquid flow model through 12.5 g of dried material after 2 minutes.

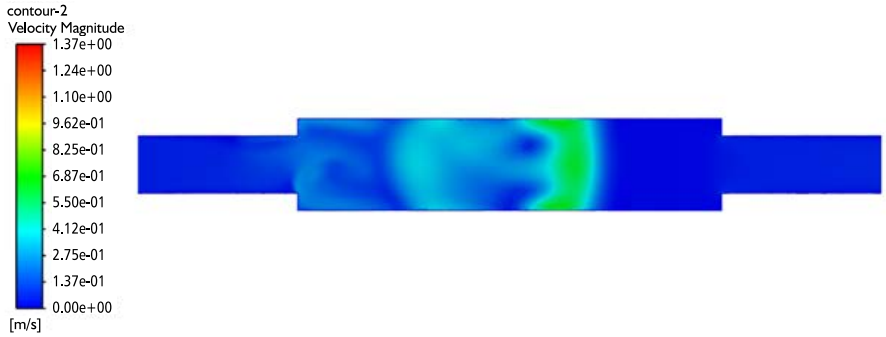

Fig. 12. Velocity magnitude distribution from numerical simulations of liquid flow model through 12.5 g of dried material after 2 minutes.

Numerical studies were also conducted for the dried material model with a mass of 12.5 g and a flow time of 10 minutes. The resulting pressure distribution is shown in Fig. 13, and the velocity magnitude distribution is shown in Fig. 14.

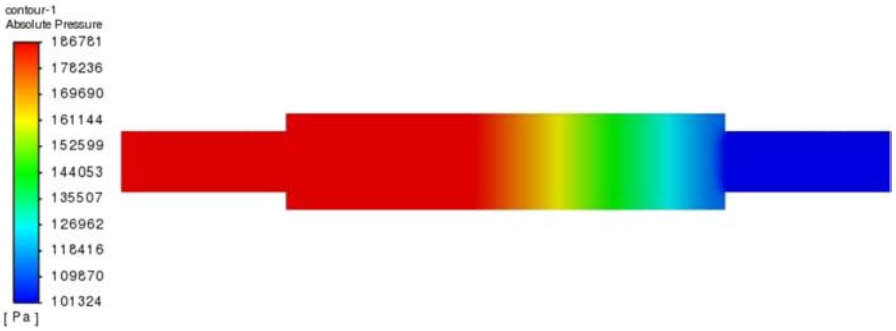

Fig. 13. Pressure distribution from numerical simulations of liquid flow through 12.5 g of dried material after 10 minutes.

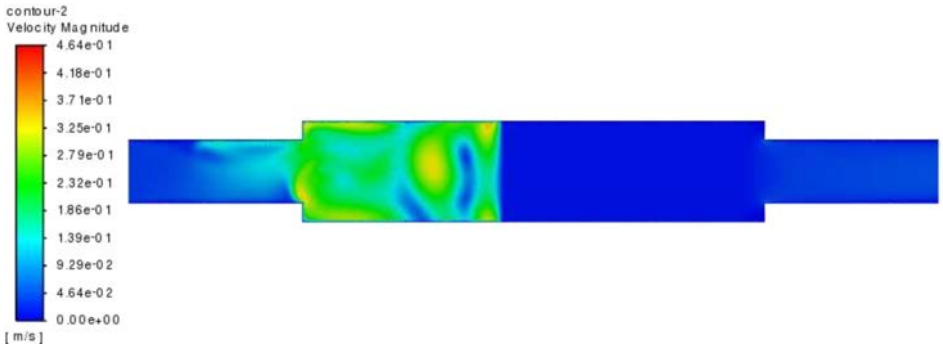

FIG. 14. Velocity magnitude distribution from numerical studies of liquid flow through 12.5 g of dried material after 10 minutes.

In the pressure distribution graph within the pipe, a region with a maximum pressure of 0.187 MPa is visible, with a pressure drop of 0.087 MPa occurring during the flow through the dried material. In terms of velocity magnitude, the maximum value reaches 0.46 m/s locally, and decreases to lower values in the section with the modeled dried material.

Based on the numerical simulations, the parameters describing the porous body model used to represent liquid flow through the dried material were determined. Table 1 presents these parameters obtained from the numerical studies.

TABLE 1. Parameters of the dried material model during liquid flow over time.

Time [min]	2			10		
Mass of dried material [g]	5	7.5	12.5	5	7.5	12.5
The resistance coefficient values [m^{-1}]	7.00E+6	7.55E+6	7.90E+6	1.07E+6	1.47E+6	1.70E+6
Mean values of the resistant coefficient [m^{-1}]	7.48E+6			1.41E+6		

The results indicate that for different times, the values of the flow resistance coefficient through the pipeline section with dried material are different. However, for the same time, the coefficient values are similar across different masses of dried material. This is especially noticeable for longer flow times. The largest differences occur during the initial phase of the flow, when the dried material undergoes volume change. For the future studies, thicker layers of dried material will be used, so it is proposed to use an average flow resistance coefficient for liquid flow through the dried material. It is assumed that these average values of the resistance coefficient will be used in subsequent numerical studies.

5. Numerical studies of the centrifugal extractor drum

The conducted experimental and numerical studies of the flow extractor were used to determine the parameters of liquid flow through material layers of specified thickness. These studies formed the basis for developing design guidelines for a centrifugal extractor. Similarly to the previous section, the numerical studies assumed the fluid as water at ambient temperature.

The model of the centrifugal extractor drum, with the section that will be filled with material, is shown in Fig. 15. The drum consists of two parts: an inner and an outer section, with the space between them filled with material. The liquid flow is directed radially outward, from the center toward the outer edge of the drum, entering the central section from the bottom. Both the inner and outer walls are made from mesh, similar to the setup used in the experimental studies. Based on this, it was assumed that the flow resistance through the mesh is negligible.

Fig. 15. Model of the centrifugal extractor drum.

Numerical simulations were conducted using the ANSYS Fluent software. The discretization of the model is one of the most important aspects of computational fluid dynamics simulations, where a properly prepared numerical mesh forms the basis for obtaining accurate flow calculations. In Fig. 16, the drum model with the applied mesh is shown. A mesh consisting of 4 432 291 elements was generated for the simulations.

The numerical simulations were conducted into two stages. In the first stage, it was assumed that the entire space inside the drum is filled with fluid flowing through the holes in the mesh separating the inner and outer sections of the drum. The simulations were carried out at rotational speeds of 250, 500, and 750 RPM.

Example results from the numerical simulations, showing the distribution of liquid flow velocity at a drum rotational speed of 750 RPM, are presented

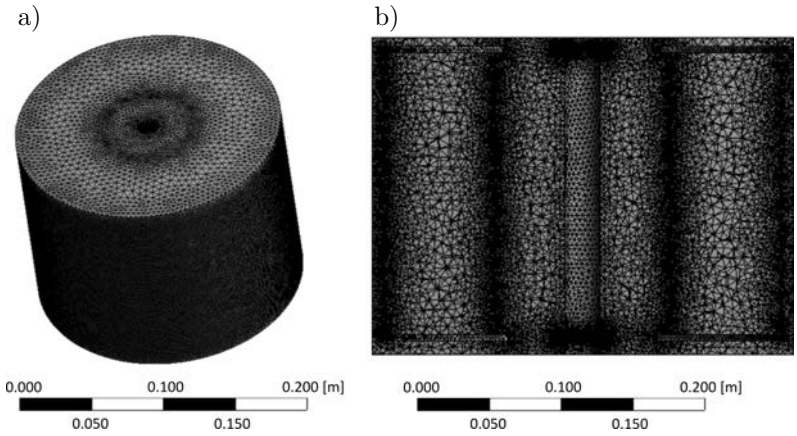

FIG. 16. The discretized model of the drum: a) external view, b) cross-sectional view.

in Fig. 17. The results are shown as a view in the cross-sectional plane. Based on the conducted numerical analysis, it can be observed that the liquid flow velocity in the radial direction is approximately 32 m/s. It can also be stated that there is no liquid movement in the vertical direction. In the case of numerical simulations at a drum speed of 500 RPM, the liquid flow velocity through the material was about 16 m/s, while at 250 RPM, the flow velocity was 7.7 m/s. The conducted research aimed to evaluate the impact of the mesh on liquid flow resistance in the centrifuge extractor drum.

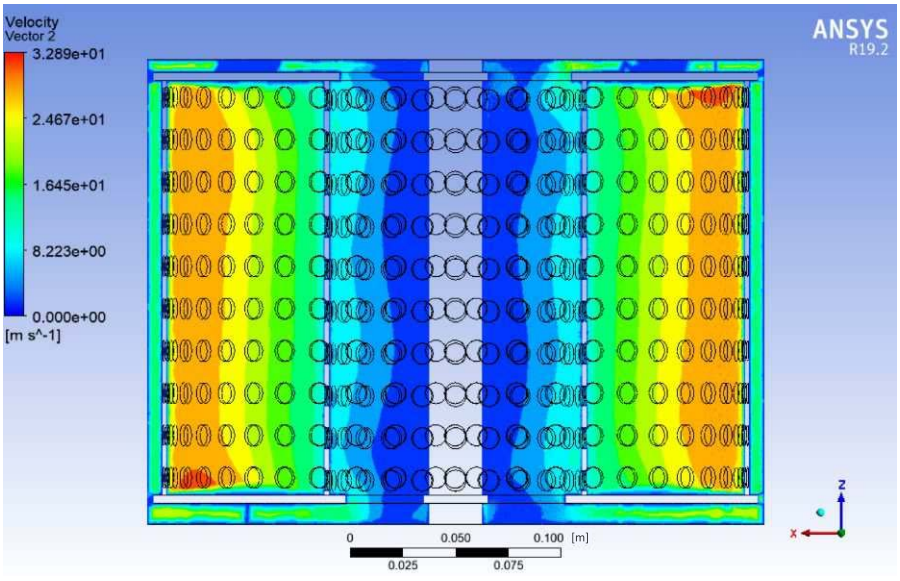

FIG. 17. Distribution of the liquid flow velocity field at a drum rotational speed of 750 RPM.

In the second stage of the numerical studies, the drum was filled with material modeled as a porous medium. Numerical analyses of liquid flow through this material were conducted at various drum rotational speeds. A liquid flow velocity of approximately 34 m/s through the material was achieved only at a drum rotational speed of 1500 RPM. Figure 18 presents the distribution of liquid velocity in the drum at this rotational speed.

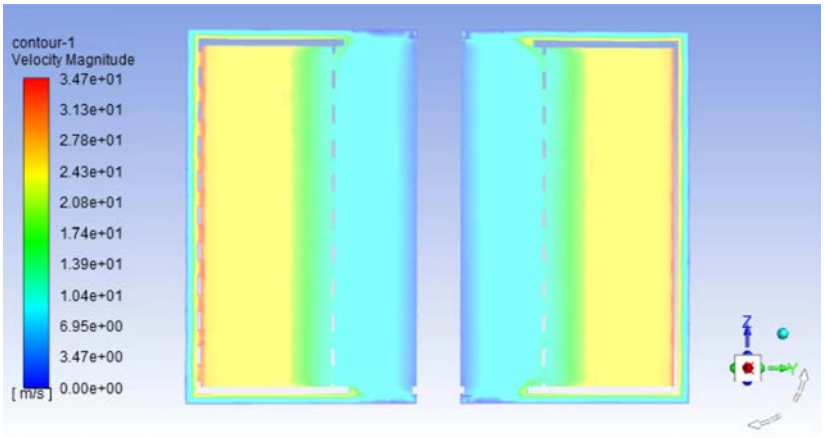

FIG. 18. Velocity field distribution of liquid flow through the material at a drum rotational speed of 1500 RPM.

Increasing the drum's rotational speed to 1500 RPM enabled achieving a liquid flow velocity through the material of approximately 30 m/s. This flow rate is considered satisfactory in light of the design requirements, which aimed to achieve a relatively high flow velocity at the lowest possible rotational speed. The results of the numerical study on liquid flow in the extractor centrifuge drum filled with material were verified using the test setup shown in Fig. 19,

FIG. 19. Test setup for studying liquid flow in the extractor drum: a) view of the setup, b) liquid flow in the drum filled with material.

where Fig. 19a presents an overall view of the setup, while Fig. 19b shows the liquid flow in the drum filled with material.

It can be observed that the liquid flow through the material is similar to the velocity distribution obtained during the numerical studies. The material moves towards the outer part of the drum under the influence of centrifugal force. This distribution of material restricts the liquid flow rate through the inner section, while increasing the liquid velocity near the outer wall.

6. Summary

This study presented the results of experimental and numerical research on the flow resistance of liquid through dried material in both flow and centrifugal extractors. The obtained results and developed research methodology were used to define key parameters for constructing a low-temperature centrifugal extractor for medicinal herbs. In the numerical studies, the dried material was modelled as a porous medium, with flow resistance parameters based on experimental data.

Based on the research, a dried layer thickness of 100 mm and a drum rotational speed of 750 RPM were determined to ensure optimal fluid flow through the test material.

The research was conducted under ambient conditions; however, the target setup requires operation at sub-zero temperatures (around -30°C) using ethanol as the solvent. Thus, further work is planned to develop a system where the solvent will be cooled, and the entire process will be conducted at sub-zero temperatures. For testing under these conditions, the laboratory setup will be reconfigured accordingly. Additional numerical studies are also planned to examine the flow resistance of liquid through the dried material at low temperatures. The ultimate outcome of this work will be to develop a low-temperature centrifugal extractor for medicinal compounds.

Funding

This project was funded by the National Centre for Research and Development under the "Path for Mazovia" competition – MAZOWSZE/0070/19.

Declaration of competing interest

The authors declare that they have no known competing financial interests or personal relationships that could have influenced the work reported in this paper.

References

1. Stepnowski P., Synak E., Szafranek B., Kaczyński Z., *Separation techniques* [in Polish: *Techniki separacyjne*], Wydawnictwo Uniwersytetu Gdańskiego, Gdańsk 2010.
2. Abubakar A.R., Haque M., Preparation of medicinal plants: Basic extraction and fractionation procedures for experimental purposes, *Journal of Pharmacy and Bioallied Sciences*, **12**: 1–10, 2020, https://doi.org/10.4103/jpbs.JPBS_175_19.
3. Borges A., José H., Homem V., Simões M., Comparison of techniques and solvents on the antimicrobial and antioxidant potential of extracts from Acacia dealbata and Olea europaea, *Antibiotics*, **9**(2): 48, 2020, https://doi.org/10.3390/antibiotics9020048.
4. Rasul M.G., Conventional extraction methods use in medicinal plants, their advantages and disadvantages, *International Journal of Basic Sciences and Applied Computing*, **2**(6): 10–14, 2018.
5. Thangjam N.M., Taijong J., Kumar A., Phytochemical and pharmacological activities of methanol extract of Artemisia vulgaris L. leaves, *Clinical Phytoscience*, **6**(1): 72, 2020, https://doi.org/10.1186/s40816-020-00214-8.
6. Zhu Z., Jiang T., He J., Barba F.J., Cravotto G., Koubaa M., Ultrasound-assisted extraction, centrifugation and ultrafiltration: multistage process for polyphenol recovery from purple sweet potatoes, *Molecules*, **21**(11): 1584, 2016, https://doi.org/10.3390/molecules21111584.
7. Meyer F., Gasimov N., Bubenheim, P., Waluga T., Concept of an enzymatic reactive extraction centrifuge, *Processes*, **10**(10): 2137, 2022, https://doi.org/10.3390/pr10102137.
8. Hamamah Z.A., Grützner T., Liquid-liquid centrifugal extractors: types and recent applications – A review, *ChemBioEng Reviews*, **9**(3): 286–318, 2022, https://doi.org/10.1002/cben.202100035.
9. Zhang Q-W., Lin L-G., Ye W-C., Techniques for extraction and isolation of natural products: a comprehensive review, *Chinese Medicine*, **13**: 20, 2018, https://doi.org/10.1186/s13020-018-0177-x.
10. Bojarska E., Cold ethanol Cannabis extraction, [in:] *19th International Technical Systems Degradation Conference*, December 14–16, 2022, Liptovsky Mikulas, pp. 120–123, 2022.
11. Mączak J., Makowski M., Samoilenko D., Rutczyńska-Wdowiak K., Initial experimental and numerical research on medical substances extractor [in Polish: Wstępne badania eksperymentalne i numeryczne ekstraktora, [in:] *Monografia: Współczesne wyzwania transportu i elektrotechniki*, No. 275, Vol. **2**, J. Wojciechowski, T. Ciszewski [Eds.], Uniwersytet Technologiczno-Humanistyczny im. Kazimierza Pułaskiego w Radomiu, pp. 95–110, 2021.
12. Mączak J., Makowski M., Bojarska E., Połaniecki A., Design and experimental study of a low-temperature flow extractor [in Polish: Budowa i badania eksperymentalne niskotemperaturowego ekstraktora przepływowego], *Przemysłchemiczny*, **103**(12): 1461–1464, 2024, https://doi.org/10.15199/62.2024.12.12.
13. Nowak A., Stachurski A., Nonlinear regression problem of material functions identification for porous media plastic flow, *Engineering Transactions*, **49**(4): 637–661, 2001, https://doi.org/10.24423/engtrans.546.2001.

14. Hassanabadi M., Akhtar S., Aune R.E., Study and modelling of fluid flow in ceramic foam filters, *Materials*, **16**(17): 5954, 2023, https://doi.org/10.3390/ma16175954.

15. Stanik M., Caban S., Klonecka M., Buczak M., Wiśniewski P., Numerical studies of internal flow in different types of filters, *Task Quarterly*, **24**(4): 335–344, 2020, https://doi.org/10.34808/tq2020/24.4/b.

16. Bae B., Jung J., Yu J.Y., Hydraulic performance and flow resistance tests of various hydraulic parts for optimal design of a reactor coolant pump for a small modular reactor, *Nuclear Engineering and Technology*, **55**(3): 1181–1190, 2023, https://doi.org/10.1016/j.net.2022.10.042.

17. Kaood A., Aboulmagd A., Othman H., El-Degwy A., Numerical investigation of the thermal-hydraulic characteristics of turbulent flow in conical tubes with dimples, *Case Studies in Thermal Engineering*, **36**: 102166, 2022, https://doi.org/10.1016/j.csite.2022.102166.

18. Tiezhu Sun T., Tang T., Ma J., Yan Y., Fu T., Zhang H., Li J., Li W., Shen H., Huan C., Experimental study on the flow resistance of inner tube and characteristics of drifting water in a tubular indirect evaporative cooler, *International Journal of Refrigeration*, **160**: 275–297, 2024, https://doi.org/10.1016/j.ijrefrig.2024.02.005.

19. Nowak R., Estimation of viscous and inertial resistance coefficients for various heat sink configurations, *Procedia Engineering*, **157**: 122–130, 2016, https://doi.org/10.1016/j.proeng.2016.08.347.

Received November 27, 2024; accepted version May 16, 2025.
Online first August 5, 2025.